ChemComm

COMMUNICATION

View Article Online
View Journal | View Issue

Cite this: *Chem. Commun.*, 2017, 53, 3713

Received 10th January 2017,
Accepted 6th March 2017

DOI: 10.1039/c7cc00193b

rsc.li/chemcomm

A switchable polymer brush system for antifouling and controlled detection†

Serkan Demirci,‡*[abc] Selin Kinali-Demirci[ac] and Shan Jiang*[bd]

A stimuli-responsive polymer brush system is designed to switch on and off surface functionality and prevent functional groups from fouling by grafting together two polymer brushes with precisely controlled lengths. The polymer brush with functional groups has a fixed length, while the other brush extends and collapses as the environment changes.

One significant challenge in biomaterial design is to combine anti-fouling properties with the functionality at the surface and interface.[1] Since many functional groups can be easily fouled when used unprotected, different chemistries have been applied to help improve the surface fouling performance, such as polyethylene glycol (PEG) and zwitterionic polymers.[2,3] They usually form a hydration layer that helps reduce foulant adsorption. However, in the meantime, anti-fouling rendition may prevent the surface from being modified to the desired properties and deteriorate the material's performance. For example, the circulation time of nanoparticles in blood can be prolonged by PEG modification. However, PEG is also known to reduce cell uptake of drug formulations which may have a negative effect on the intracellular delivery efficacy.[4] Another example is zwitterionic polymers, which can effectively prevent protein fouling. However, it remains challenging to modify the polymers and introduce surface functionality while keeping the antifouling properties.[5]

Here we adopt a different approach and address the challenge of surface fouling using stimuli-responsive polymer brushes without sacrificing the surface functionality. Two polymer brushes of different lengths are grafted together on the surface. One polymer brush is stimuli-responsive and its thickness changes as the environment changes. The other polymer brush is fixed in length and modified with functional groups. When fully extended, the stimuli-responsive polymer brush is longer than the polymer brush modified with the functional groups. Under such conditions, the surface functional groups are "switched off" and shielded from fouling. When the stimuli-responsive polymer brush collapses and becomes shorter than the polymer brush modified with functional groups, the functionality is "switched on". By shielding the surface functionality when not in use and only exposing it when needed, the fouling can be drastically reduced.

The key to the success of this design is to precisely control the length of the polymer brush. The polymer brush has been widely investigated and applied in a broad range of applications including filtration, separation, biosensors, tissue engineering, and drug delivery.[6–8] Recent advances in polymer chemistry enabled the synthesis of polymer brushes with well-defined architecture and length, such as nitroxide-mediated radical polymerization, atom-transfer radical polymerization (ATRP), reversible addition–fragmentation chain transfer (RAFT) polymerization, and single electron transfer-living radical polymerization (SET-LRP).[9–13] Taking advantage of these different polymerization techniques, both RAFT and SET-LRP were applied in our study to synthesize a binary mixture of polymer brushes with precisely controlled lengths.

In addition, cyclodextrins (CDs)[14,15] were applied to functionalize the polymer brushes. CDs are cyclic oligosaccharides consisting of (1,4)-linked glucopyranose units having a truncated cone-shaped molecular structure. Through the host–guest supramolecular interaction, CDs offer a versatile means to interact with a wide variety of molecules.[16,17] These supramolecular systems have played a significant role in many applications ranging from agriculture to biotechnology.[18–21] In addition, CD-functionalized materials can provide high separation or purification performance and can be used for the removal of organic molecules from liquid and vapour phases.[22–24] However, CD molecules can also be easily

[a] *Department of Chemistry, Iowa State University, Ames, IA 50011, USA. E-mail: srkndemirci@gmail.com, sdemirci@iastate.edu*
[b] *Materials Science and Engineering, Iowa State University, Ames, IA 50011, USA. E-mail: sjiang1@iastate.edu*
[c] *Department of Chemistry, Amasya University, Amasya 05100, Turkey*
[d] *Division of Materials Science & Engineering, Ames National Laboratory, Ames, Iowa 50011, USA*

† Electronic supplementary information (ESI) available. See DOI: 10.1039/c7cc00193b

‡ SD conceived the idea. SD and SKD designed and performed the experiments. SD and SJ co-wrote the manuscript. All authors have given approval to the final version of the manuscript.

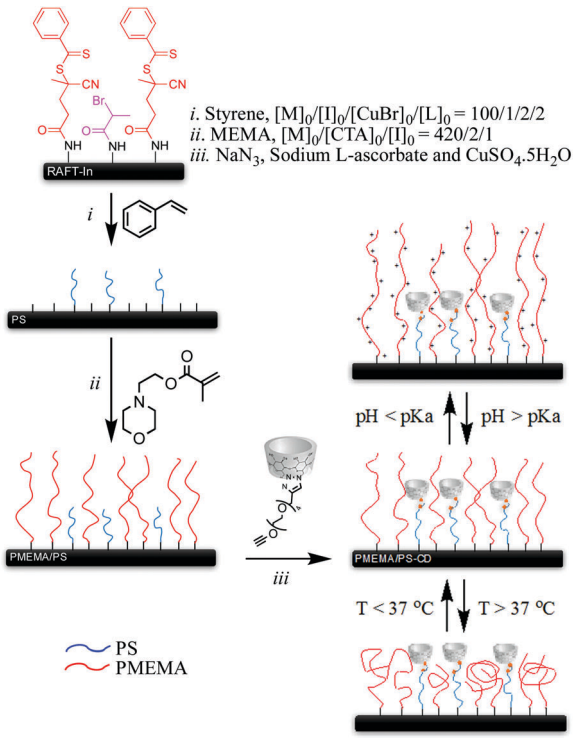

Scheme 1 Preparation of the CD-functionalized polymer brushes.

fouled when exposed to contaminants. To protect CD molecules against undesirable interactions, a series of poly(2-*N*-morpholinoethyl methacrylate) (PMEMA) chains with different lengths were synthesized. The modified surface was characterized by XPS, FTIR, ellipsometry and AFM. In addition, pH- and thermo-responsive properties were investigated by contact angle measurements. The FITC–Ada molecule was used to optimize the polymer brush system for fouling protection and controlled detection. Aniline was used as a contaminant to examine the fouling performance. The optimized polymer brush system was further functionalized to detect the hepatitis C virus.

Scheme 1 shows the fabrication of the two polymer brushes on the surface. Starting from the silicon wafer, PMEMA was synthesized through RAFT polymerization while the polystyrene (PS) brush was synthesized *via* SET-LRP. The prepared PMEMA/PS surface was then functionalized with tetraethylene glycol modified CD, which was synthesized *via* a click reaction. For more details, please refer to the ESI.† The RAFT agent/initiator ratio was calculated as 3.44 from the XPS survey spectrum. In addition, the PMEMA/PS/CD molar ratio was determined as 3.13/1.09/1 from the high resolution XPS spectra of C 1s.

As shown in Scheme 1, the obtained surface can respond to both pH and temperature changes. When the pH is higher than the pK_a, PMEMA becomes charged, and the electrostatic repulsion helps extend the polymer chains. Also because of the charge, the surface becomes relatively hydrophilic. On the other hand, when the temperature decreases, PMEMA tends to form more hydrogen bonding within the polymer chains, which will lead to the collapse of the polymer brush and expose the more

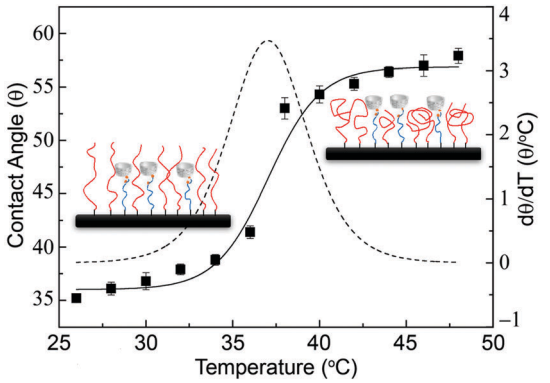

Fig. 1 Temperature-dependence of water contact angles of the PMEMA/PS brush and a derivative curve of dθ/dT *versus* T (pH = 7).

hydrophobic moiety to the surface. This change is clearly demonstrated in Fig. 1, as the temperature sweeps from 25 °C to 50 °C, the contact angle changes from 35° to 57° with a transition temperature of ~37 °C. The surface pK_a value for the CD-functionalized polymer brushes was determined as 5.3 through contact angle measurement as shown in Fig. S18 (ESI†).

When extended PMEMA chains are long enough, they can effectively shield CDs on the PS chain. However, in order to expose the CD groups on the PS brush when the PMEMA brush collapses, the polymer chains also have to be short enough. As a result, PMEMA chains need to be precisely controlled and fine-tuned for the purpose of effectively turning on and off the surface functionality. The molecular weight of the polymer brush was characterized by gel permeation chromatography (GPC) while the dry thickness of the polymer brush was measured by ellipsometry. According to previous studies,[25,26] the molecular weight of the grafted polymer chains is similar to that of the free polymer chains in solution. Fig. 2 shows clearly that as polymerization progresses, the molecular weight keeps increasing. From the slope of the linear curve, the grafting density of PS and PMEMA/PS surfaces, σ (chains per nm^2), was estimated to be 0.21 and 0.61 chains per nm^2, respectively. The grafting density and the polymer R_g calculation suggest that the PMEMA/PS layer is densely packed and adopted the stretched brush confirmation.[11] In addition, the

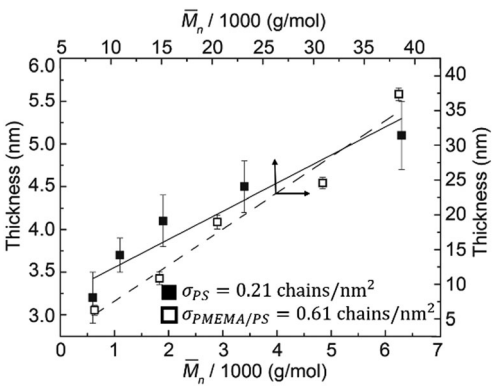

Fig. 2 Evolution of ellipsometric thickness h (nm) of the PS and PMEMA/PS chains as a function of $\bar{M}_{n,GPC}$.

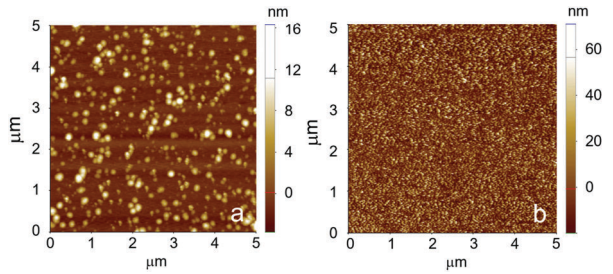

Fig. 3 AFM images of PS (a) and PMEMA/PS (b).

thickness of the polymer brush is proportional to the molecular weight of the polymer chains.

Fig. 3 shows the AFM images of the polymer brush grafted onto a silicon wafer. Fig. 3a shows that PS forms islands on the substrate due to the relatively low grafting density. It is also speculated that under such conditions PS may adopt a mushroom morphology. After grafting with PMEMA, the grafting density becomes much denser. The polymer chains may now adopt the extended brush geometry.

The FITC–Ada molecule was used as a target molecule, which can interact with CD and label the polymer brush. The optimum initial concentration of FITC–Ada and the adsorption time were determined as 25 μM and 24 h, respectively (Fig. S22, ESI†). The substrate was carefully conditioned and rinsed before and after immersion in a solution of FITC–Ada. The fluorescence intensity of the substrate corresponds to the extent of the interaction of CD with FITC–Ada. In our polymer brush system, high intensity means that CD is fully exposed to and interacted with FITC–Ada, while low intensity means that CD is shielded from FITC–Ada. The same procedure was repeated at both 25 °C and 40 °C in a series of experiments to determine the optimized chain length combination of the polymer brushes. In this experiment, the length of PS was fixed, while the length of PMEMA was gradually increased as the polymerization time increases.

As shown in Fig. 4, when the PMEMA length is relatively short (polymerization time <8 h), even at 25 °C when PMEMA chains are extended, they cannot effectively shield the PS chains and CD molecules. As a result, the fluorescence intensities at both 25 °C and 40 °C are high. As the PMEMA chain length increases (polymerization time ~8–16 h), the fluorescence intensity gradually decreases at 25 °C, which suggests that PMEMA starts to shield CD molecules on the PS chains. When the PMEMA length is long enough, the fluorescence intensity at 25 °C stays low (polymerization time of 8 h). On the other hand, when the PMEMA length is too long (polymerization time of 16 h), the fluorescence intensity at 40 °C is also low, which suggests that PMEMA is longer than PS even after PMEMA collapsed. Based on the results, the polymerization time of 8 h for MEMA is selected for further experiments. Under this condition, the average molecular weight $\bar{M}_{n,GPC}$ equals 30 900 g mol^{-1} ($\bar{M}_{n,NMR}$ = 31 600 g mol^{-1}), and PDI is 1.11.

With the optimized polymer brushes, the fouling of the PMEMA/PS-CD wafers was tested using aniline vapour as the fouling source. The detection capability afterwards was further measured by the adsorption of phenolphthalein in aqueous solution. First, PMEMA/PS-CD wafers were exposed to 5 mL aniline in a sealed desiccator. The exposure time was varied between 1 and 28 days at both 24 °C and 40 °C. After the exposure, the silicon wafers were removed from the desiccator and immersed for 12 h in phenolphthalein solution (0.1 M), which was adjusted to pH 7.4 by addition of PBS buffer solution. The depletion of phenolphthalein from the solution was then determined by UV-vis spectrophotometry at 562 nm.

As shown in Fig. 5, during the exposure to aniline vapour, if CD is well protected or shielded by PMEMA (24 °C and pH < pK_a), the fouling is considerably less, which will lead to high adsorption and low C/C_0 values in the subsequent phenolphthalein solution. On the other hand, when CD is unprotected (40 °C and pH > pK_a), the fouling is much higher and the subsequent adsorption of phenolphthalein is lower, which will lead to a high C/C_0 value. The results shown in Fig. S23 (ESI†) clearly demonstrate that a polymer brush system can effectively lower the fouling of the surface functional groups when the protection is switched on during the fouling experiment.

The reusability of the PMEMA/PS-CD surface was investigated by measuring the adsorption of FITC–Ada through immersion and sonication cycles. As shown in Fig. S23 (ESI†), FITC–Ada desorbed after sonication cleaning at 45 °C. The immersion/sonication cycle was repeated up to five times, and the switchable polymer brush surface can still be reused after cleaning.

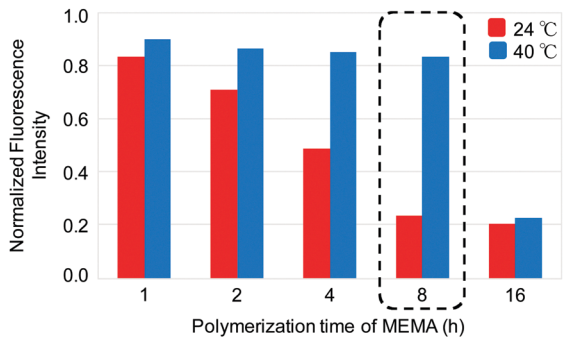

Fig. 4 Fluorescence intensity of CD-functionalized PMEMA/PS surfaces with a fixed PS, $\bar{M}_{n,GPC}$ of 6300 g mol^{-1} ($\bar{M}_{n,NMR}$ = 6150 g mol^{-1}) and various polymerization times of MEMA.

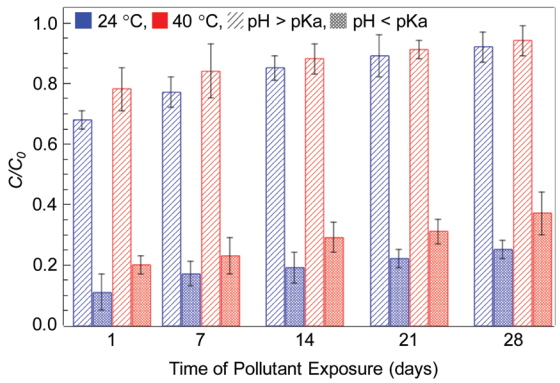

Fig. 5 C/C_0 as a function of exposure time, where C_0 and C are the concentration of the phenolphthalein solution before and after the adsorption.

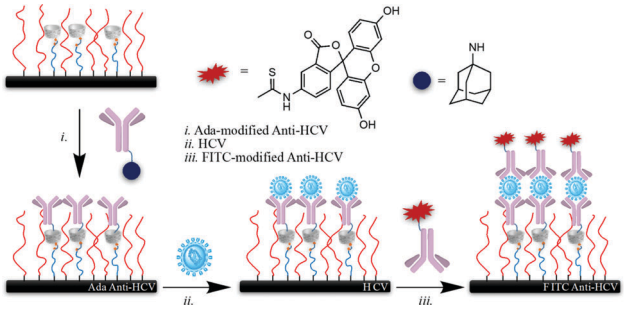

Scheme 2 Illustration of host–guest interaction between the target molecule and PMEMA/PS-CD used for HCV detection.

Fig. 6 Fluorescence microscopy images and fluorescence intensities for each of the three steps in the preparation of PMEMA/PS-CD for detecting HCV.

To further demonstrate the concept, the PMEMA/PS-CD was applied to detect the HCV. Before the detection, the surface can be stored at 25 °C where PMEMA chains are extended to protect the CD molecules from fouling. The first step in activating the surface for HCV detection is to modify the CD molecules under the right conditions. As shown in Scheme 2, CD-functionalized polymer brushes were first immersed in the solution of Ada grafted anti-HCV molecules at 40 °C for 24 h (PBS, pH = 7.4), where PMEMA chains collapsed and CD is exposed. The same polymer brushes optimized in the previous experiment using FITC–Ada were used here to ensure that CD–Ada interaction is not impeded. Then these prepared substrates were reacted with HCV at 36 °C for 1 h. Afterwards the surface was labeled using FITC conjugated anti-HCV. Fig. 6 shows the fluorescence images and intensities of the substrate in each step of the surface treatment. Fluorescence from FITC labelling is clearly visible.

HCV detection is one example that demonstrates the feasibility of potential applications of the polymer brush system. The detection may be further optimized by adjusting the concentration and incubation time. This new system can work for the detection of many other molecules based on antigen–antibody interactions. The advantage here is the capability of protecting the surface functionality when not in use and initiating the detection through stimuli-responsive polymers.

In summary, we successfully designed a polymer brush system that can switch surface functionality on and off upon exposure to environmental stimuli. A CD-functionalized binary polymer brush system (PMEMA/PS) was successfully prepared *via* a combination of SET-LRP, RAFT polymerization, and click chemistry. FTIR, XPS, ellipsometry and AFM further confirmed the surface structure and morphology change after the modification. Static water contact angle measurements indicated the wetting–dewetting transition of the PMEMA/PS surface at a transition temperature of 37 °C. The chain length of PMEMA and PS was optimized to protect and de-protect CD molecules. The fouling behaviour of the PMEMA/PS surface was tested using aniline vapour. The optimized surface was finally functionalized for HCV detection. These results demonstrate that fouling and the undesirable interactions of the CD molecules can be prevented by switching on the PMEMA brush protection. This provides an effective way to store the functional groups when not in use, and prolong the shelf life of the functional surface. In addition, this new strategy offers alternative ideas for combining the anti-fouling property and surface functionality without compromising the performances. The same polymer brush design can be further applied to many other systems, including functionalized nanoparticles, stimuli-responsive self-assembly, and controlled release drug delivery systems.

This work was supported in part by The Scientific and Technological Research Council of Turkey – TUBITAK (Project # 112T868) and the start-up funds provided by Iowa State University.

Notes and references

1 C. Blaszykowski, S. Sheikh and M. Thompson, *Biomater. Sci.*, 2015, **3**, 1335–1370.
2 Q. Shao and S. Jiang, *Adv. Mater.*, 2015, **27**, 15–26.
3 B. Cao, L. Li, H. Wu, Q. Tang, B. Sun, H. Dong, J. Zhe and G. Cheng, *Chem. Commun.*, 2014, **50**, 3234–3237.
4 A. A. D'souza and R. Shegokar, *Expert Opin. Drug Delivery*, 2016, **13**, 1257–1275.
5 S. C. Lange, E. van Andel, M. M. Smulders and H. Zuilhof, *Langmuir*, 2016, **32**, 10199–10205.
6 N. Ayres, *Polym. Chem.*, 2009, **1**, 769–777.
7 R. Barbey, L. Lavanant, D. Paripovic, N. Schüwer, C. Sugnaux, S. Tugulu and H.-A. A. Klok, *Chem. Rev.*, 2009, **109**, 5437–5527.
8 M. Krishnamoorthy, S. Hakobyan, M. Ramstedt and J. Gautrot, *Chem. Rev.*, 2014, **114**, 10976–11026.
9 W. Li, C. Bao, R. Wright and B. Zhao, *RSC Adv.*, 2014, **4**, 18772–18781.
10 A. Nese, Y. Kwak, R. Nicolaÿ, M. Barrett, S. Sheiko and K. Matyjaszewski, *Macromolecules*, 2010, **43**, 4016–4019.
11 S. Demirci and T. Caykara, *React. Funct. Polym.*, 2012, **72**, 588–595.
12 D. Cimen and T. Caykara, *Polym. Chem.*, 2015, **6**, 6812–6818.
13 S. Demirci, S. Kinali-Demirci and T. Caykara, *J. Polym. Sci., Part A: Polym. Chem.*, 2013, **51**, 2677–2685.
14 J. Deng, X. Liu, W. Shi, C. Cheng, C. He and C. Zhao, *ACS Macro Lett.*, 2014, **3**, 1130–1133.
15 Y. Zhang, L. Ren, Q. Tu, X. Wang, R. Liu, L. Li, J.-C. Wang, W. Liu, J. Xu and J. Wang, *Anal. Chem.*, 2011, **83**, 9651–9659.
16 J. Szejtli, *Chem. Rev.*, 1998, **98**, 1743–1754.
17 A. Hedges, *Chem. Rev.*, 1998, **98**, 2035–2044.
18 J. Shi, Z. Chen, B. Wang, L. Wang, T. Lu and Z. Zhang, *ACS Appl. Mater. Interfaces*, 2015, **7**, 28554–28565.
19 E. M. M. Valle, *Process Biochem.*, 2003, **39**, 1033–1046.
20 X. Ma, N. Zhou, T. Zhang, Z. Guo, W. Hu, C. Zhu, D. Ma and N. Gu, *RSC Adv.*, 2016, **6**, 13129–13136.
21 T. Uyar, R. Havelund, J. Hacaloglu, F. Besenbacher and P. Kingshott, *ACS Nano*, 2010, **4**, 5121–5130.
22 A. Celebioglu, S. Demirci and T. Uyar, *Appl. Surf. Sci.*, 2014, **305**, 581–588.
23 N. Morin-Crini and G. Crini, *Prog. Polym. Sci.*, 2013, **38**, 344–368.
24 A. Celebioglu, H. Sen, E. Durgun and T. Uyar, *Chemosphere*, 2016, **144**, 736–744.
25 M. Baum and W. J. Brittain, *Macromolecules*, 2002, **35**, 610–615.
26 M. Barsbay, O. Güven, M. H. Stenzel, T. P. Davis, C. Barner-Kowollik and K. Barner, *Macromolecules*, 2007, **40**, 7140–7147.

